Structures 33 (2021) 2811–2823

Contents lists available at ScienceDirect

Structures

journal homepage: www.elsevier.com/locate/structures

The effect of furnace steel slag powder on the performance of cementitious mortar at ambient temperature and after exposure to elevated temperatures

Md Jihad Miah [a], Md. Kawsar Ali [a], Francesco Lo Monte [b], Suvash Chandra Paul [c], Adewumi John Babafemi [d], Branko Šavija [e,*]

[a] Department of Civil Engineering, University of Asia Pacific, Dhaka-1205, Bangladesh
[b] Department of Civil and Environmental Engineering, Politecnico di Milano, Piazza Leonardo da Vinci 32, 20133 Milan, Italy
[c] Department of Civil Engineering, International University of Business Agriculture and Technology, Dhaka 1230, Bangladesh
[d] Department of Civil Engineering, Stellenbosch University, Private Bag X1, Matieland 7602, Stellenbosch, South Africa
[e] Microlab, Faculty of Civil Engineering and Geosciences, Delft University of Technology, 2628CN Delft, the Netherlands

ARTICLE INFO

Keywords:
Induction furnace steel slag powder
Mortar
Shrinkage
Strength
Durability
Elevated temperatures

ABSTRACT

Induction furnace steel slag is a secondary product obtained when molten steel is separated from the impurities in the steel-producing furnaces. Though numerous studies have been published on the mechanical strength of concrete/mortar made with steel slag as fine aggregate, relatively few studies focus on the shrinkage, durability (i.e., porosity, water absorption, and resistance to chloride penetration) at ambient temperature, and especially the mechanical and durability performances after exposure to elevated temperatures. Within this context, the present study investigates mechanical strength, shrinkage, and durability of mortar made with different contents of steel slag powder (SSP) at two different water-to-cement (w/c) ratios before and after exposure to elevated temperatures (120, 250, 400 and 600 °C). Mortars made with SSP showed significantly higher mechanical strength and better durability than mortar made with 100% natural sand (control mortar). Compressive, tensile, and flexural strength increased by 45%, 72% and 56%, respectively, when SSP entirely replaced natural sand. Porosity, water absorption, and chloride penetration decreased by 42%, 61% and 52%, respectively, for 100% SSP mortar. Furthermore, the shrinkage of the mortar decreased with increasing percentages of SSP. Conversely, residual compressive strength after heat exposure was lower for 100% SSP mortar than for the control mortar. Therefore, this study presents a first step towards the successful utilization of SSP in cementitious mortar.

1. Introduction

With the reprocessing of industrial waste and secondary industrial products as raw construction materials (such as induction furnace steel slag), the concrete industry can contribute to sustainable development, bringing considerable environmental benefits. This aspect can be very important, considering that concrete is the most used construction material globally, with more than 4 billion tons of cement produced per year.

These byproducts can be used to (partly) replace fine or coarse aggregate or, in some cases, even part of the cement as a binder. Regarding fine aggregate, it is well known that they allow to reduce the cost of concrete, on the one hand, and to bring in important benefits in terms of time-dependent (such as shrinkage and creep) and mechanical properties [1], even though their relative volume in the concrete mix is usually just around 20–30% [2].

Fine aggregate is generally made by natural sand (NS), mostly dredged from the riverbeds. Due to the global rise of construction activity, the demand for concrete is continuously increasing, particularly in developing economies. In some cases, this can lead to problems in the supply chain: for example, in the Netherlands, the supply of natural fine aggregates is becoming limited [3]. In this regard, finding possible alternatives to limited natural resources is important. Using steel slag as an aggregate in concrete is additionally appealing, considering that the demand for other construction materials such as steel and iron is increasing (with more than 1.8 billion tons of steel produced per year in the world), thus resulting in increased generation of waste from the production process. If part of this waste would be used to replace NS in

* Corresponding author.
E-mail addresses: jihad.miah@uap-bd.edu (M. Jihad Miah), Francesco.lo@polimi.it (F. Lo Monte), suvashpl@iubat.edu (S. Chandra Paul), ajbabafemi@sun.ac.za (A. John Babafemi), b.savija@tudelft.nl (B. Šavija).

https://doi.org/10.1016/j.istruc.2021.06.047
Received 5 December 2020; Received in revised form 25 May 2021; Accepted 16 June 2021
2352-0124/© 2021 The Author(s). Published by Elsevier Ltd on behalf of Institution of Structural Engineers. This is an open access article under the CC BY license (http://creativecommons.org/licenses/by/4.0/).

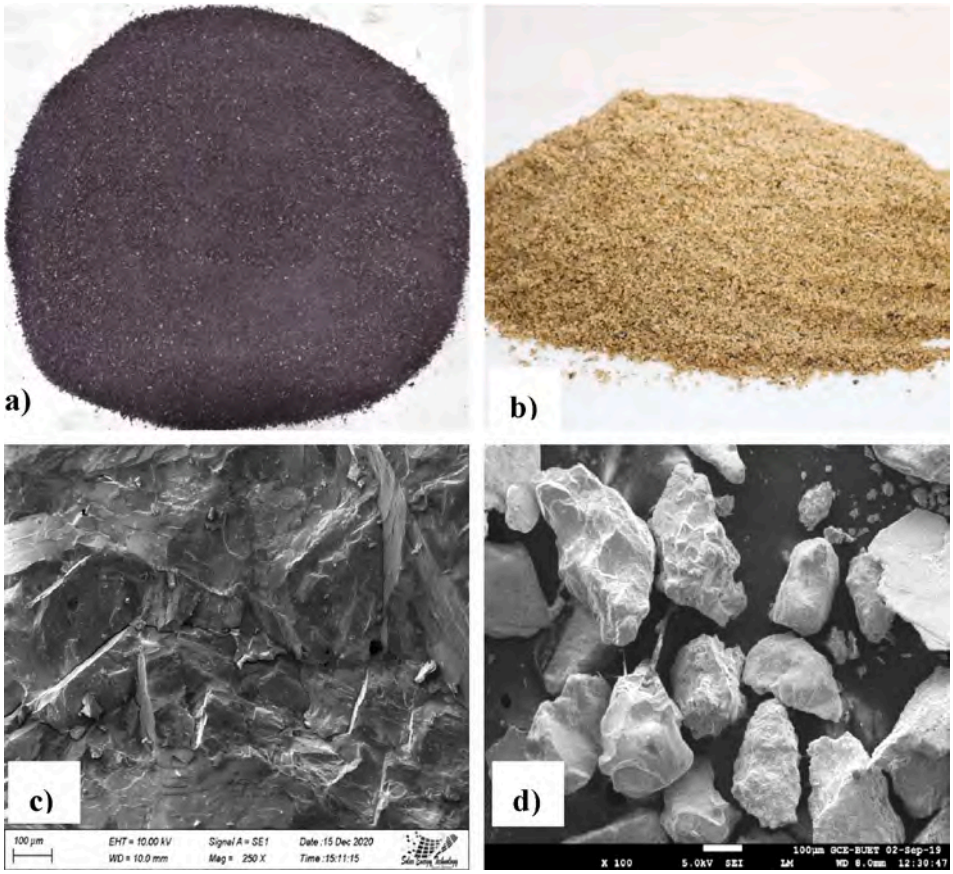

Fig. 1. Pictures of Steel Slag Powder - SSP (a) and Natural Sand - NS (b), and SEM images of SSP and NS (c-d).

concrete, this would (1) partly relieve the need for its disposal, (2) lower new aggregates demand, and (3) reduce the overall demand for cost and energy.

One of the byproducts of the steel-making process is steel slag. Some studies have shown that it can replace natural coarse aggregate in concrete [4–7] or even part of the cement as a binder. Other studies have shown that steel slag fine aggregate (SSFA) improves concrete performance and allows a general reduction of carbon footprint and impact on the environment [7–10]. The literature has reported increases by 1.1–1.3 and 1.4–2.4 times in compressive and tensile strength, respectively, of concrete made with SSFA [9]. The optimum replacement ratio of sand by SSFA was identified as 15–30% for compressive and 30–50% for tensile strength, respectively. However, a decrease in concrete workability was found by introducing SSFA because of the increased amount of finer particles and the angular shape of the SSFA compared to sand. Devi and Gnanavel [11] confirmed this trend. They reported that the compressive and flexural strength increased by up to 40% upon replacement of NS by SSFA, though accompanied by a consequent decrease in workability. Similar results were reported by Qasrawi et al. [9], who also found that concrete made with 40% SSFA showed higher resistance to HCl and H_2SO_4 compared to the control mix. The benefits of using SSFA in concrete (by partially or fully replacing natural sand) in terms of strength, toughness, and energy absorption capacity have also been reported in other studies [12–15]. Furthermore, due to the higher specific gravity of slag, concrete density is usually increased, which could make such concrete more effective in special applications such as radiation shielding [16].

Fire can cause severe damages (e.g., cracks, ruptures and explosive spalling, etc.) or even drive to the failure of the entire concrete structures, which could raise the risk of people's lives and economic loss. Fire significantly diminishes the stiffness, strength properties (by increasing permeability, porosity, and decomposition of binder hydrated minerals) and provokes concrete spalling, which seriously jeopardizes the integrity of the entire concrete structure [17–18]. Roy et al. [19] reported that concrete made with Electric Arc Furnace (EAF) fine aggregate had an inferior fire performance compared to concrete made with NS in terms of mechanical behavior, especially when exposed to temperatures above 500 °C. On the other hand, Rashad et al. [20] reported an improvement in the compressive strength after exposure to elevated temperatures (200, 400, 600 and 800 °C) when GBFS is used to replace NS in alkali-activated slag mortars. The residual tensile ad flexural strength of mortar made with waste steel slag (WSS) and waste clay brick (WCB) were investigated after exposure to elevated temperatures (up to 600 °C). The mortar specimens were made with 50% and 100% replacement of NS by WSS and WCB. The strength tests of mortar specimens were performed at 90 days [21]. The strength of the mortar decreased as the temperature increased. A significant strength loss was observed for the specimens heated at 600 °C, and both residual tensile and flexural strength reduction was more for the mortar made with WSS and WCB than NS. Further research is, therefore, needed to elucidate the effect of cementitious materials with steel slag as fine aggregate exposed to elevated temperatures.

A literature study reveals that most published studies have focused on the mechanical response of concrete/mortar incorporating steel slag as fine aggregate. In contrast, very limited research has been devoted to its shrinkage, durability (i.e., total porosity, capillary water absorption, and chloride penetration resistance) at ambient temperature and mechanical strength and porosity performances after exposure to elevated temperatures (120, 250, 400 and 600 °C). Therefore, the current study addresses the physico-mechanical behavior of cementitious mortars made with SSP as partial/full replacement for NS at ambient temperature and after heat exposure. As the safety of people inside a building

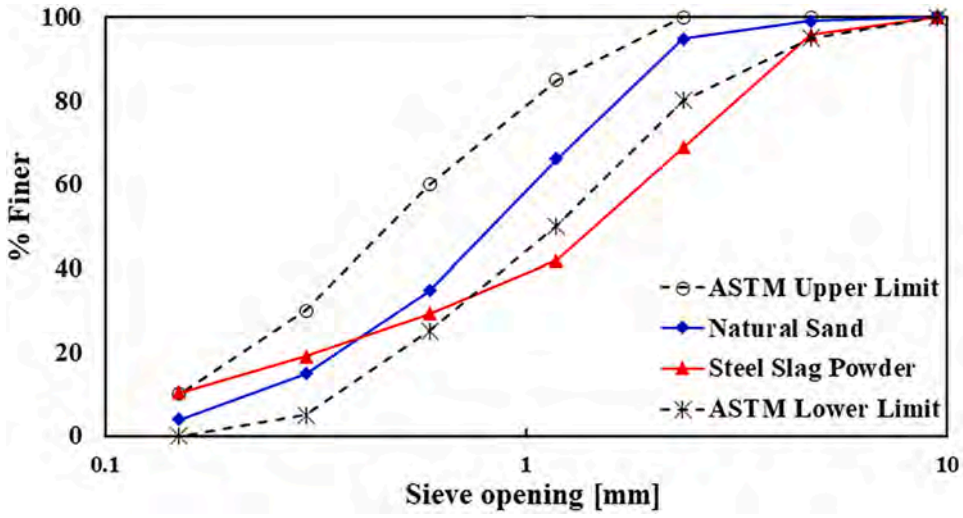

Fig. 2. Grading curves of NS and SSP compared with the upper and lower limits recommended by ASTM C33 [23].

Table 1
Physical properties of the fine aggregates used in this study.

ID	Fineness modulus	Specific gravity	Absorption capacity [%]
NS	2.86	2.56	5.9
SSP	3.35	3.24	1.0

Table 2
Oxide compositions of cement and steel slag powder (SSP).

Oxide composition	Cement [%]	SSP [%]
CaO	53.43	4.94
SiO_2	24.90	26.18
Al_2O_3	7.52	4.94
Fe_2O_3	3.96	44.39
MgO	2.52	0.47
MnO	0.07	12.9
SO_3	4.77	0.43
TiO_2	1.18	1.73
K_2O	1.00	0.56
Na_2O	0.27	0.45
P_2O_5	0.21	0.08
SrO	0.08	0.09
ZrO_2	0.01	0.11

structure is of utmost importance during an unexpected fire, it is essential to have comprehensive knowledge about the fire response of the cementitious mortar made with SSP to ensure stable fire resistance of the structural elements.

2. Experimental methodology

2.1. Mortar mixes and fine aggregate characterization

The materials used to prepare mortar mixes comprised cement (CEM II 42.5 N), water, and SSP, NS or a combination of both as fine aggregate (Fig. 1a-b). The natural sand was received from the market, commonly collected by dredged from ocean and river beds. While, the SSP was produced during mechanically crushing the solid steel slag boulders to produce steel slag coarse aggregate, and this waste powder was used as a replacement for NS in this study. Scanning Electron Microscopy (SEM) was used to investigate the microscopic morphology of SSP and NS, and the resulting SEM images are shown in Fig. 1c-d. SSP appears highly angular with a rough surface texture obtained from steel slag chunk crushing [6].

Table 3
Mortar mix designs used in this study (all quantities in kg/m^3).

	Mix ID	Cement	Aggregates		Water
			NS	SSP	
w/c = 0.3	SSP 0%	811	1216	0.0	243
	SSP 25%	811	912	385	243
	SSP 50%	811	608	770	243
	SSP 75%	811	304	1155	243
	SSP 100%	811	0.0	1540	243
w/c = 0.5	SSP 0%	545	1362	0.0	272
	SSP 25%	545	1021	431	272
	SSP 50%	545	681	862	272
	SSP 75%	545	340	1293	272
	SSP 100%	545	0.0	1724	272

Both NS and SSP were sieved with an ASTM standard No. 4 sieve (4.75 mm aperture) [22], showing the particle size distribution reported in Fig. 2 (bounded by the limits provided by the ASTM C33 [23]). Table 1 shows the main properties of NS and SSP tested following ASTM C128 [24]. As shown in Table 1, SSP has higher specific gravity than NS, while its absorption capacity is lower. Grading curves of NS and SSP (Fig. 2) show that SSP is characterized by a higher content of smaller (from 0.15 to 0.074 mm) and bigger size particles (from 1.18 to 4.75 mm) compared to NS. On the other hand, for the intermediate size, the grading curve of SSP falls below the lower limit proposed by ASTM 33 [23]. It is to be expected that the increased amount of smaller particles will fill the micropores of the cementitious matrix, thereby densifying the microstructure and consequently result in improved strength and durability.

Table 2 shows the oxide composition of SSP determined using X-ray fluorescence (XRF). As expected, the Fe_2O_3 content of SSP was considerably higher, resulting in a higher specific gravity with respect to NS (see Table 1).

Ten different mortar mixtures have been designed, with two w/c ratios (0.30 and 0.50) and five levels of NS replacement by induction furnace SSP (0%, 25%, 50%, 75% and 100%). Superplasticizer (Sika-Plast® – 204 TH) was used in the content of 0.5% wt. of cement in the case of w/c equal to 0.30 to increase mortar workability. The mix design of the mortar mixes is given in Table 3.

2.2. Experimental program and test procedures

The study was undertaken in two parts: (i) determination of mechanical and durability properties at ambient conditions and (ii)

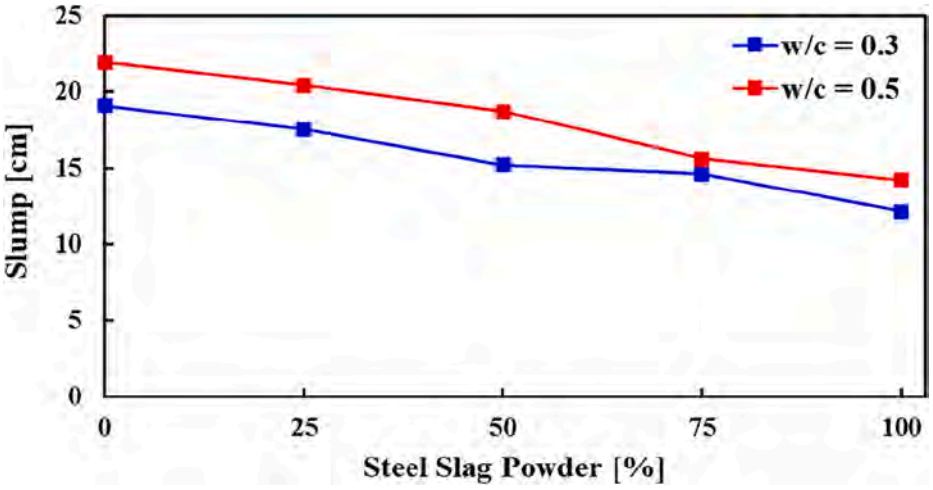

Fig. 3. Slump of fresh mortar mixes made with different percentages of SPP.

assessing the influence of high temperature on compressive strength and porosity. The details are described below.

2.2.1. Characterization at ambient temperature

Fresh property

Slump values (as a measure of workability) of fresh mortar before casting test specimens were measured by investigating the viability of the mortar mixes (using an inverted cone under the action of gravity) for all replacement levels of NS by SSP.

Mechanical properties

For all the mortar mixes, compressive, tensile, and flexural strengths were determined at ambient temperature, according to ASTM C109

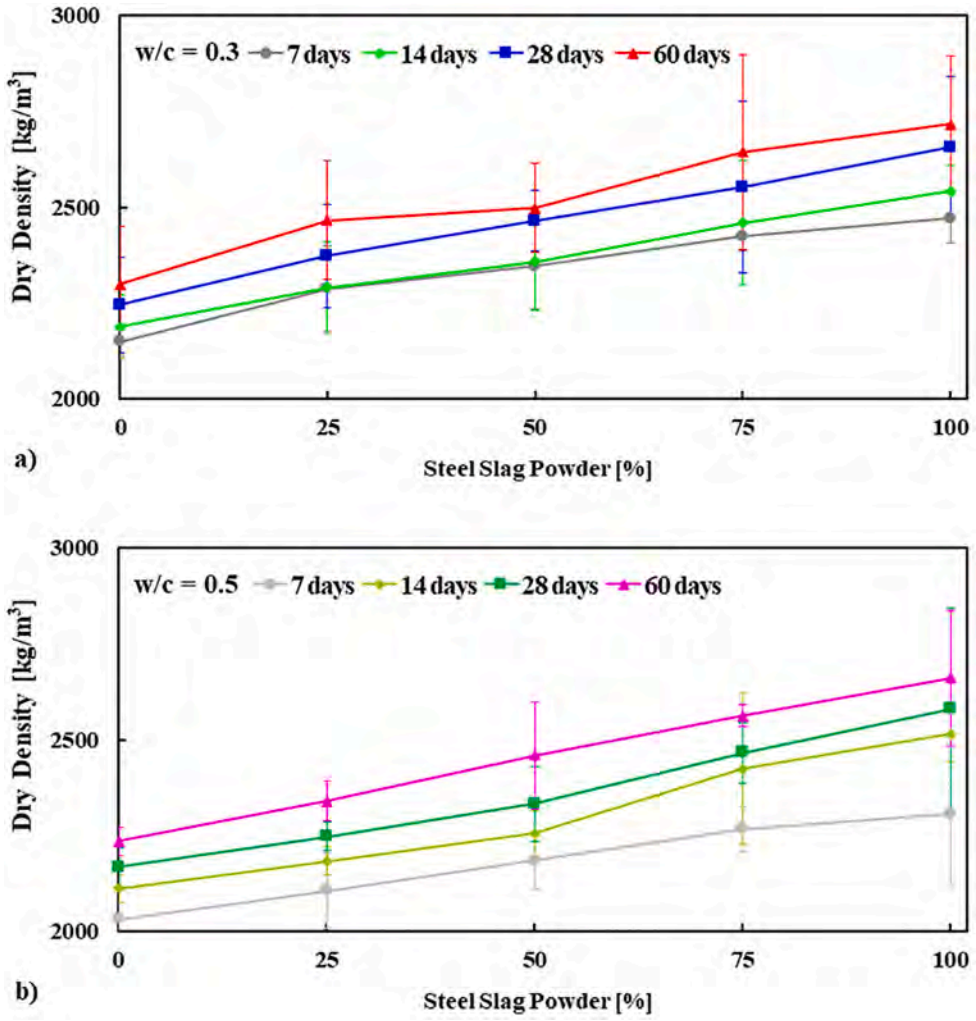

Fig. 4. Dry density of mortar made with two water-cement ratios (w/c) of 0.3 (a) and 0.5 (b) at different percentages of SSP.

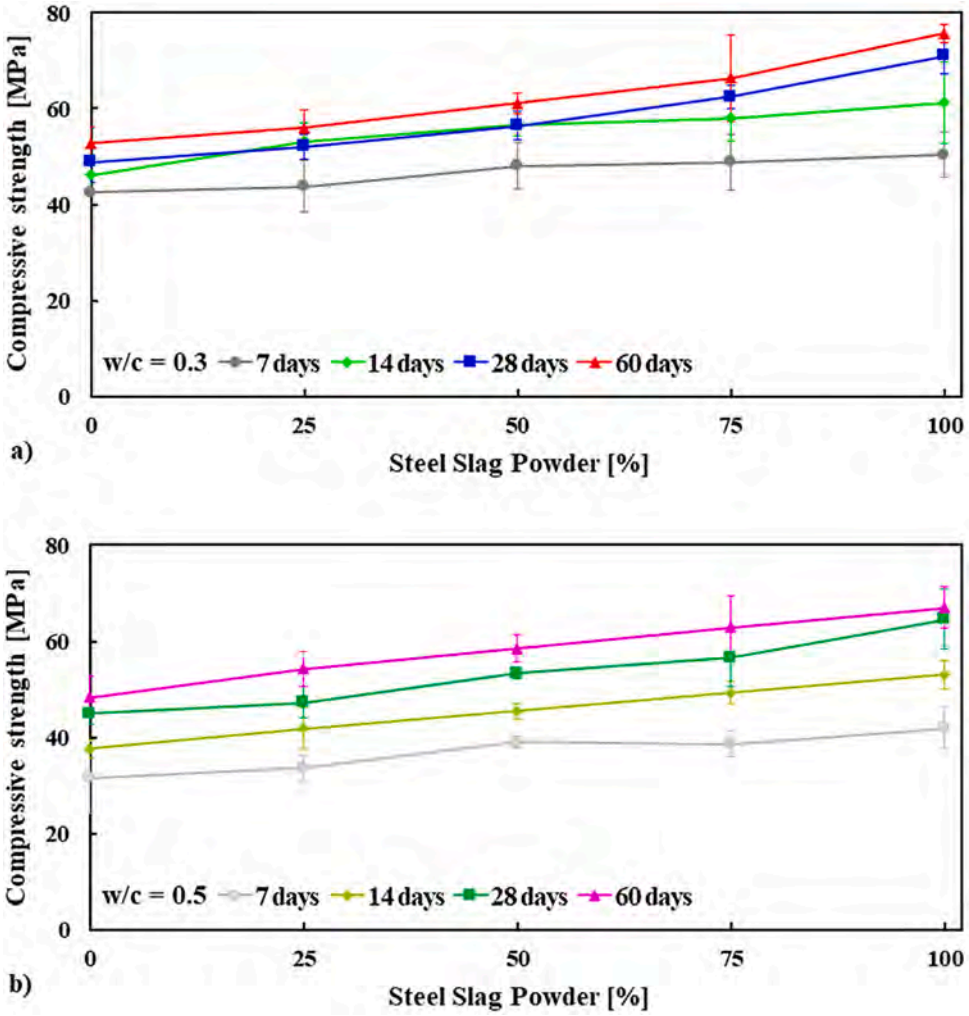

Fig. 5. Compressive strength of mortar specimens made with w/c of 0.3 (a) and 0.5 (b) tested at 7, 14, 28 and 60 days.

[25], ASTM 307 [26], and ASTM 348 [27], respectively, at 7, 14, 28 and 60 days from casting.

The dry density of each specimen was measured before compressive strength tests. In addition, autogenous shrinkage was measured for all mortar mixes (on specimens 25 mm × 25 mm × 285 mm) according to ASTM C 490 [28].

Durability

The overall durability performance of the mortar mixes was characterized by measuring their porosity, water absorption, and resistance to chloride penetration. Three specimens were used for each mix, and the average result was evaluated.

Porosity was investigated via water absorption porosity according to French standard NF P18–459 [29], capillary water absorption was determined as indicated in AFPC–AFREM [30] (with mass measurement of specimens recorded up to 120 h until a constant mass was achieved). At the same time, a chloride penetration resistance test was conducted according to ASTM C1202 [31].

2.2.2. *Characterization after exposure to elevated temperature*

The detrimental effect of heat exposure has been investigated in residual conditions by heating the specimen at the heating rate of 2 °C/min up to the target temperature (120, 250, 400 and 600 °C). Once the target temperature was reached, it was maintained for 28, 10, 4 and 4 h, respectively, to attain stability [32] in the mortar. Subsequently, the furnace was allowed to cool down to room temperature before the specimens were taken out. The control tests were performed at 20 °C after 90 days from casting to determine the reduction of compressive strength due to elevated temperature. Furthermore, the residual porosity of mortar specimens was also evaluated using the same procedures described for room temperature.

3. Results and discussion

3.1. *Workability*

The workability of the fresh mortar mixes measured using the Slump Test is presented in Fig. 3. As the percentage of SSP increases, the workability of fresh mortar decreases, down to a reduction of about 35% when SSP fully replaced the NS. This agrees with other studies in the literature [9,11]. The significant decrease of the slump flow can be explained by the highly angular and rough surface texture of SSP (see Fig. 1b-c). This results in the decreased mobility of the fresh mortar due to better particle interlocking.

On the contrary, NS is relatively round, thereby enhancing the flowability due to the rolling effect. Besides, the reduction in slump could also be attributed to the higher percentage of bigger particles (from 1.18 to 4.75 mm, see Fig. 2) of SSP with respect to NS. It was found that SSP particles retained on the sieve opening of 4.75 mm, 2.36 mm and 1.18 mm were 10, 12.5 and 1.9 times higher than NS. Furthermore, the fineness modulus (FM) of SSP and NS were 3.35 and 2.86, respectively.

The combination of higher coarser particles and higher FM could

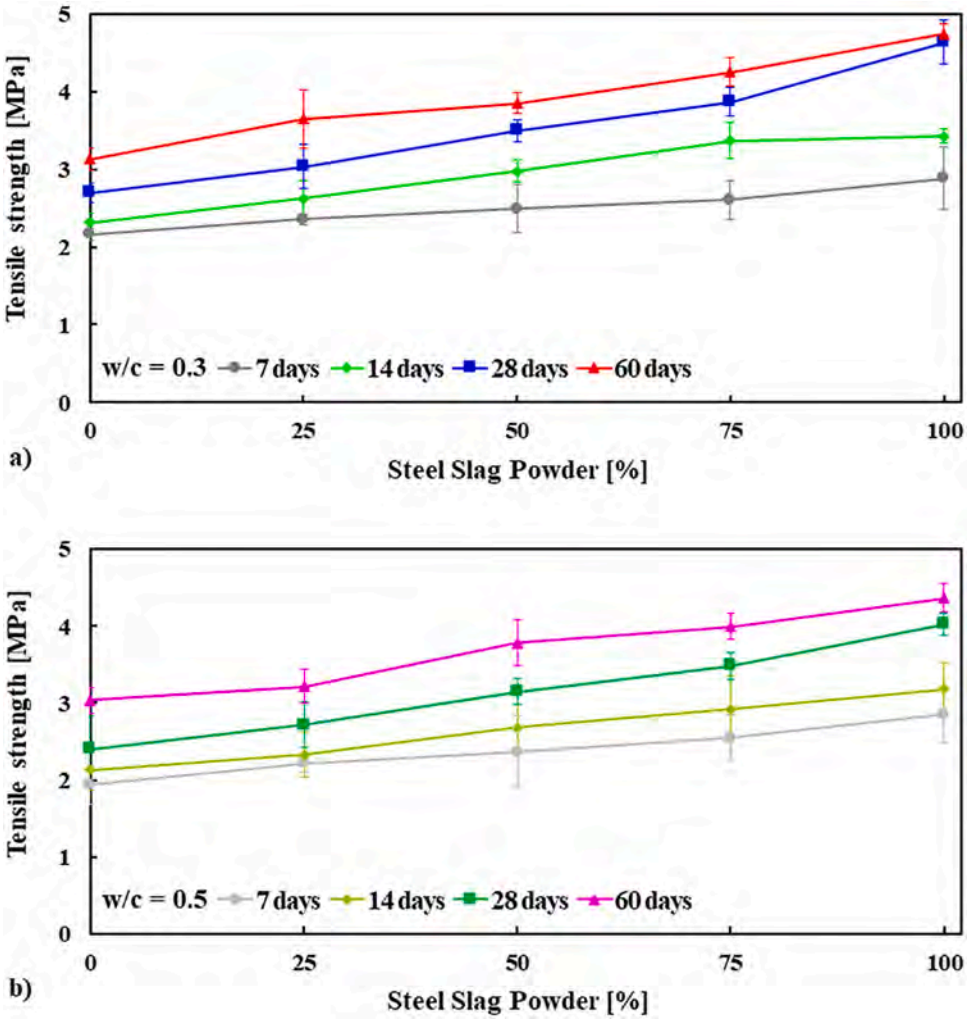

Fig. 6. Tensile strength of mortar specimens for w/c ratio of 0.3 (a) and 0.5 (b) tested at 7, 14, 28, and 60 days.

induce higher friction among the particles in the mortar mix with SSP. Similar trends of the slump with respect to SSP content were observed for w/c of 0.3 and 0.5 (see Fig. 3).

3.2. Physico-mechanical properties at ambient temperature

3.2.1. Dry density

Fig. 4 shows the average density of the hardened mortar as a function of SSP content. As expected, with increased SSP content, an increase in the dry density at both w/c ratios was observed due to the higher specific gravity of SSP (28% higher than NS). As expected, the highest mortar density was achieved with 100% SSP, with a 14–19% increase over the reference at all ages. Similar results are also reported by other researchers [9,10,14].

3.2.2. Compressive strength

Compressive strength (f'_c) of mortars at 7, 14, 28 and 60 days is presented in Fig. 5. The results illustrate that cementitious mortars made with SSP as fine aggregate have a significantly higher compressive strength than the mortar made with 100% NS (control specimen). For example, the mean compressive strength for w/c ratio of 0.30 at 28 days for mixes with 0%, 25%, 50%, 75% and 100% SSP contents were 48.9 MPa, 52.1 MPa, 56.4 MPa, 62.4 MPa and 71.0 MPa, respectively. At the same SSP contents, the strength is 45.0 MPa, 47.3 MPa, 53.3 MPa, 56.5 MPa and 64.5 MPa, respectively, for a w/c ratio of 0.50. Therefore, an increase in the range of 19–45% was observed for the mortar made with 100% SSP at all curing ages with respect to the control specimen. The increase is attributed to the higher content of finer particles (from 0.074 mm to 0.15 mm) than NS, fostering a denser microstructure. Furthermore, SSP used in the present study was a crushed-coarser particle with rough surface texture and angular shape (see Fig. 1). These properties may enhance the strength of the interfacial transition zone (ITZ) between the cement paste and the aggregate, resulting in a strength increase in cement-based composites [33,34].

Furthermore, the higher strength of mortar made with SSP could also be partially explained by the pozzolanic nature of SSP that reacts with calcium hydroxide [$Ca(OH)_2$] and then forming secondary calcium silicate hydrate (CSH) gels. Such behavior has been reported by Santamaría-Vicario et al. [10].

3.2.3. Tensile and flexural strength

Fig. 6 shows tensile strength at 7, 14, 28 and 60 days. It can be seen that the incorporation of SSP leads to a significant increase in tensile strength at all curing ages. These results are consistent with the results of compressive strength (see Fig. 5). The maximum strength was attained for SSP relative content of 100%, which increased by 72% for w/c ratio of 0.30, and 68% for w/c of 0.50 with respect to the control mortar at 28 days. Compared to compressive strengths, the relative increase in terms of tensile strength is higher.

The flexural strength of mortar mixes made with SSP is presented in Fig. 7. Similar to tension, the flexural strength of mortar mixes with SSP was significantly higher for all curing ages than the control mortar. The

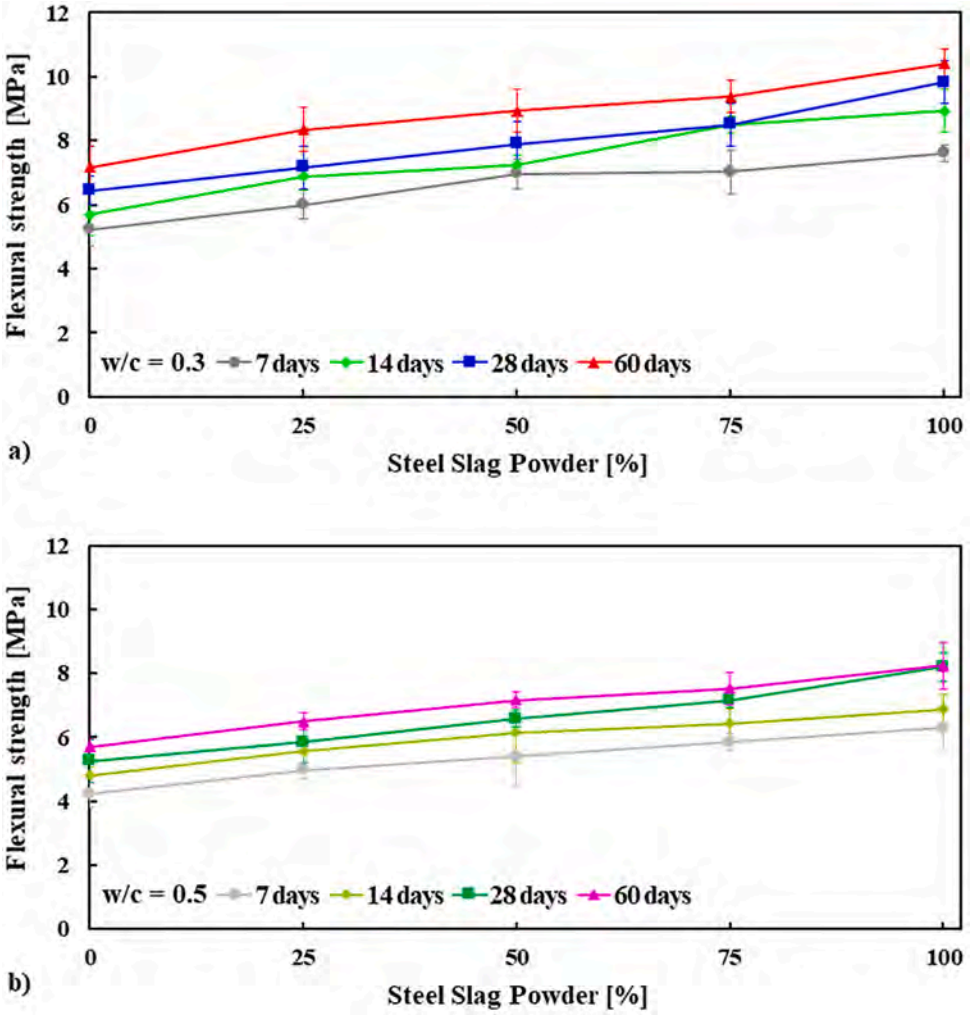

Fig. 7. Flexural strength for w/c ratio of 0.3 (a) and 0.5 (b) at 7, 14, 28 and 60 days.

most remarkable improvement was observed for the mortar made with 100% SSP, which showed about 43–57% higher strength than the control mortar for both w/c and all curing ages. As previously noted, this is related to the denser matrix, the better aggregate-cement ITZ, and the higher angularity of the SSP particles.

As previously noted, this is related to the denser matrix and the better aggregate-cement ITZ of mortar made with SSP than NS. It should be noted that the particle shape of NS is almost rounded (because NS is received from riverbeds and uncrushed) and less angular (see Fig. 1b and d). On the contrary, the SSPs are highly angular, dense, and have an

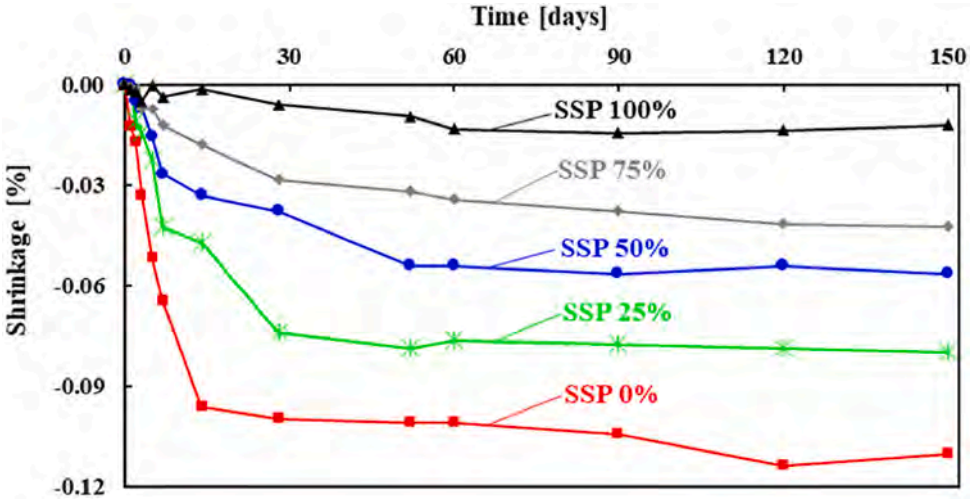

Fig. 8. Shrinkage as a function of time for w/c ratio of 0.30.

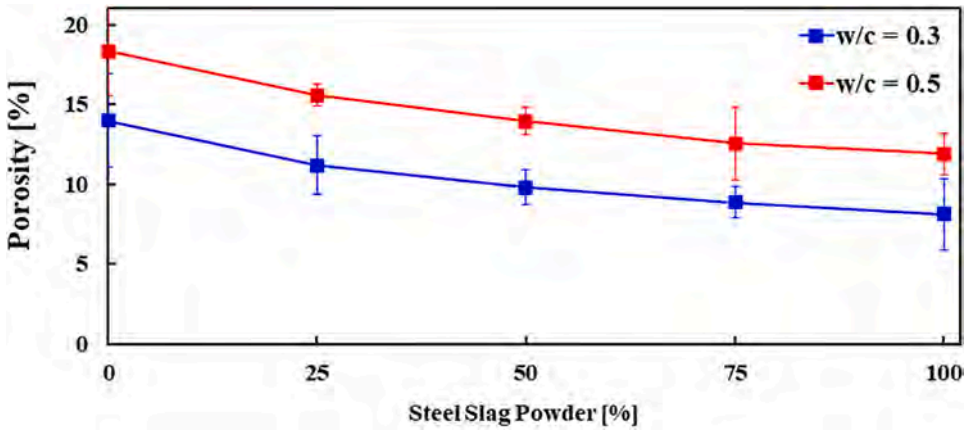

Fig. 9. Porosity for w/c ratio of 0.30 and 0.50 at 28 days.

excellent rough surface texture due to the crushing of solid steel slag boulders (see Fig. 1a and c). This allows better ITZ than NS, resulting in higher mechanical strength. Moreover, as mentioned earlier, the higher mechanical strength of mortar made with SSP could also be the contribution of the secondary CSH gels produced by the pozzolanic reaction of SPP [10], which is believed to be the strength-giving compound of the binder. Indeed, SPP particles might have an adequate specific surface area to allow pozzolanic responses. It contains a significantly higher finer particle content (from 0.074 mm to 0.15 mm and even smaller, thus rest on the Pan of the ASTM Sieve, see Fig. 2) than NS.

Lower w/c ratios lead to higher strength for all curing ages and SSP relative contents. On the other hand, it is worth noting as the variation of the strength with the relative content of SSP is not significantly dependent on the initial w/c ratio.

3.2.4. *Shrinkage*

Autogenous shrinkage has been monitored overtime for all the mixes with a w/c ratio of 0.30, and the results are presented in Fig. 8, where

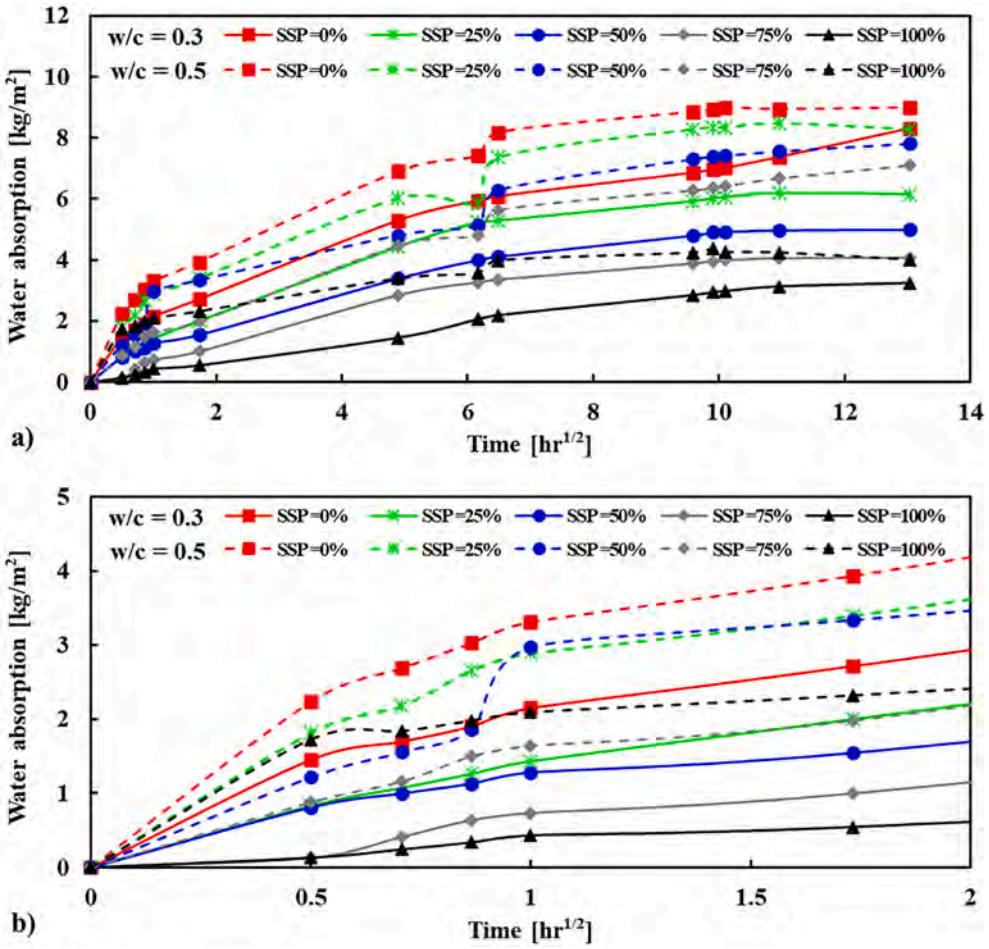

Fig. 10. Capillary water absorption (a) and detail in data near the origin to represent the slope of the curves (b) of mortar specimens made with w/c ratios of 0.30 and 0.50.

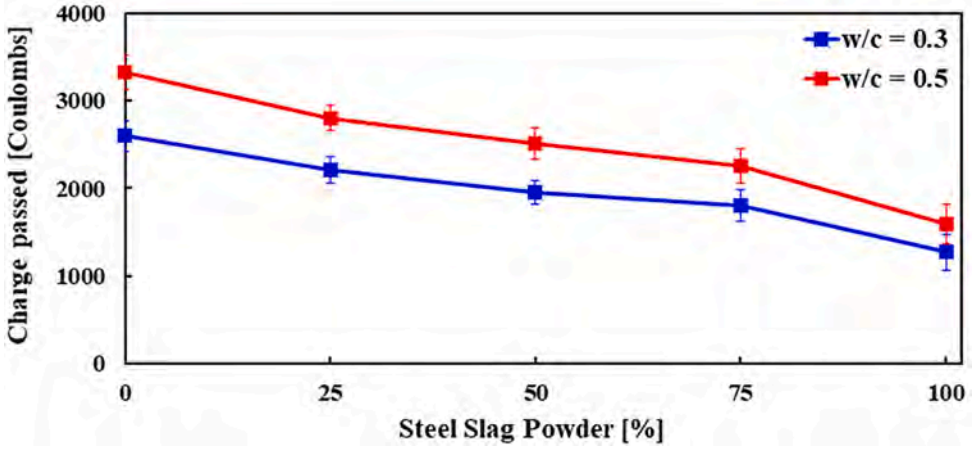

Fig. 11. Charge passed, a measure of chloride resistance, for different mortar mixtures.

the average of three specimens is shown. It can be observed as shrinkage decreases significantly with SSP, especially at a higher content. Specimens with 100% SSP show a 94% reduction at 28 days and 89% at 150 days than to control mortar. Such a decrease can be ascribed to two main reasons. On the one hand, the higher water absorption capacity [35] of NS than SSP (5.9% for NS and 1% for SSP, see Table 1), leading to a larger absorption of water from the capillary pores of the cement paste. On the other hand, the higher angularity of SSP particles more effectively restrain the shrinkage of the matrix.

3.3. Durability

3.3.1. Porosity

The total porosity of mortar has been measured at 28 days to investigate the role of SSP, and the results are shown in Fig. 9. The apparent porosity of mortar regularly decreases with increasing replacement percentages of NS by SSP for mortar mixes at both w/c ratios. This is consistent with the higher strength of the latter (see Fig. 5, Fig. 6 and Fig. 7). The maximum decrease in porosity was determined in the mortar with 100% SSP, which was 42% lower than the control mortar for w/c of 0.30 and 35% for a w/c ratio of 0.50. The reduction in porosity can be explained by the significant reduction of the micropores within the range from 74 μm to 150 μm, and also for lower dimensions. As described in Section 3.2.2, a higher quantity of finer particles (lower than 0.15 mm, see Fig. 2) is present in SSP thereby filling the micropores with a resultant lower porosity.

3.3.2. Capillary water absorption

The effect of SSP on the capillary water absorption (WA) of mortar is shown in Fig. 10a, with the details of data points near the origin representing the slope of the curves shown in Fig. 10b. Water absorption decreases for increasing values of SSP relative content. A notable depletion in water absorption was observed for the mortar mixes made with 75% and 100% SSP (see Fig. 10b). Water absorption decreased at 170 h by 61% for a w/c ratio of 0.30 and 55% for a w/c ratio of 0.50, when SSP entirely replaced NS. These results agree with the results of total porosity (see Fig. 9).

As previously discussed, this could be due to significantly lower absorption of SSP and denser microstructure in the matrix, particularly the ITZ. These results imply that the use of SSP as fine aggregate enhances the resistance against water penetration, which can improve the corrosion resistance. Similar trends have been observed for both w/c ratios, even though lower water absorption values have been obtained for all mortar mixes in the case of w/c ratios of 0.3, as expected.

3.3.3. Resistance to chloride penetration

Fig. 11 shows the resistance of mortars to chloride penetration. As can be seen, the use of SSP as a replacement of NS significantly improves chloride penetration resistance of mortar mixes since the transmitted charge was decreased for increasing contents of SSP. The mortar mix made with 100% SSP had the lowest charge transmission. The average charge passed into mortar specimens made with 0%, 25%, 50%, 75% and 100% SSP were 2595C, 2207C, 1959C, 1806C and 1271C, respectively, for w/c of 0.30 and 3327C, 2805C, 2517C, 2257C and 1589C, for w/c of 0.50. The results indicate that the chloride ion permeability ranges from moderate (0% to 25% SSP mortar for w/c of 0.30 and 0% to 75% SSP mortar for w/c of 0.50) to low (50% to 100% SSP mortar for w/c of 0.30 and 100% SSP mortar for w/c of 0.50) level according to ASTM C1202 [31]. The average current passing through mortar with 100% SSP was 52% lower than the control mortar. This means that the inclusion of SSP in mortar as fine aggregate enhances the resistance against chloride penetration, which could provide good protection to steel reinforcement against corrosion. These results are consistent with the other parameters investigated. Such lower chloride penetration of mortar made with SSP can be ascribed to the denser microstructure.

3.4. Compressive strength and porosity after exposure to high temperature

3.4.1. Residual compressive strength

The effect of high temperature on the decay of compressive strength is shown in Fig. 12a for all the mortar mixes, while the normalized compressive strength is presented in Fig. 12b and c. The experimental results are compared with the curves recommended by Eurocode 2 [36] and ACI 216–1.07 [37], which, however, refers to concrete. A monotonic decrease with temperature has been observed for all the mixes, and except for 100% SSP specimens, the results are within limits indicated by Eurocode 2 [36] and ACI 216–1.07 [37]. At 120 °C, the strength decreased by 2–7% for w/c ratios of 0.30 and 0.50 compared to the strength in virgin conditions (without thermal treatment). The evaporation of free water and part of the physically bound water is the cause of the reduction in strength at this temperature due to porosity increase (see next section) [32,38]. This is in good agreement with Miah et al. [32], where a sharp increase in permeability in the temperature range of 80–120 °C. Similar behavior was also reported by Kalifa et al. [39] and Bazant [40].

At 250 °C, the strength dropped gradually for each mix. A sharper decrease was observed for the mortar mixes made with 100% SSP. The residual strength for mortar with 0%, 25%, 50%, 75 and 100% were 86%, 85%, 82%, 78% and 74%, respectively, at w/c ratio of 0.30. At a w/c ratio of 0.50, residual strengths were 88%, 85%, 84%, 81% and 78% compared to ambient temperature. The results agree with the concept that denser matrices usually show a sharper decrease of strength with the temperature [41]. This is due to the increase of vapor pressure in the pores [42] on the one hand, and the decrease of the transient thermal

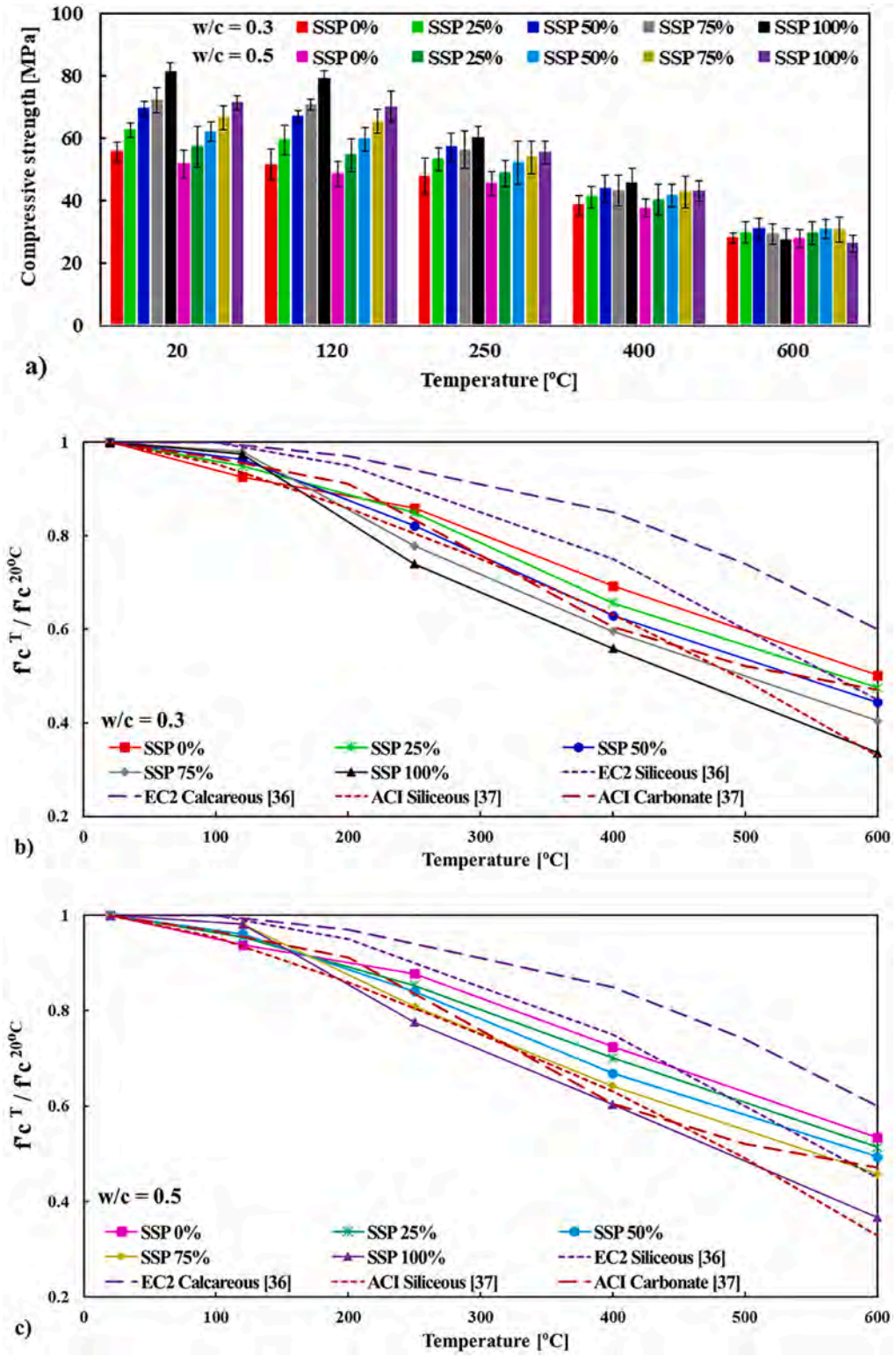

Fig. 12. Residual compressive strength (a) and normalized strength at w/c of 0.3 (b) and w/c of 0.5 (c), for all mortar mixes after exposure to high temperatures, together with the recommendation provided by Eurocode 2 (EC 2) [36] and ACI 216–1.07 [37].

strain, on the other hand. Lower transient thermal strain means higher apparent stiffness at high temperature, thus higher thermal stresses. The combined effect of higher pore pressure and higher thermal stresses brings in more severe cracking of the specimen during heating, with a consequent lower strength in residual conditions.

From 400 to 600 °C, strength dropped sharply, reaching a reduction with respect to virgin conditions of 69–34% for w/c ratio of 0.30 (see Fig. 12b) and 72–37% for w/c ratio of 0.50 (see Fig. 12c). This can be attributed to the significant loss of water from gel pores, dehydration, increase of porosity and permeability [39]. Besides, strength reduction could be due to atmospheric moisture absorption and rehydration of lime (CaO) during cooling, resulting in the higher cracking caused by an increase in volume [43].

The reduction of strength resulting from exposure to high

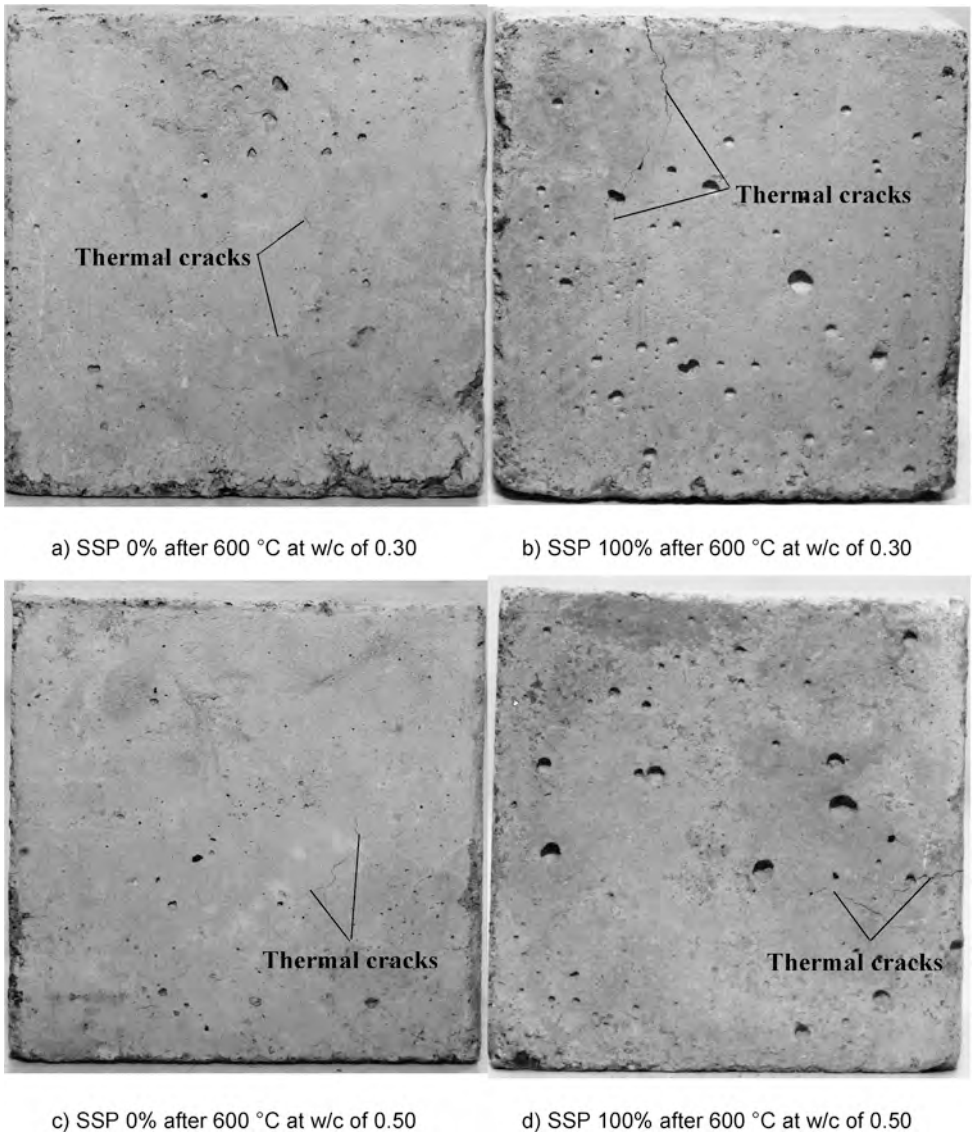

Fig. 13. Images of mortar specimens made with 0% and 100% SSP at w/c of 0.30 and 0.50 after exposure to 600 °C.

temperature was higher for the mortar mixes with SSP at both w/c ratios. For instance, the loss in strength for mortar with 100% NS and 100% SSP exposed to 600 °C were 50% and 66%, respectively, at a w/c ratio of 0.30, and 47% and 63%, accordingly, at a w/c ratio of 0.50. The higher reduction in strength for the mortar with 100% SSP can be ascribed to the following reasons: (a) significantly higher initial compressive strength (compressive strength for mixes with 100% NS and with 100% SPP was 55.76 MPa and 81.31 MPa for w/c of 0.30 and 51.78 MPa and 71.47 MPa, accordingly, for w/c ratio of 0.50) and (b) the presence of bigger size particles (from 1.18 to 4.75 mm) in SSP aggregates (see Fig. 2). When the mortar is exposed to high temperatures, the cement paste shrinks due to water loss while aggregates expand due to thermal dilation [32,39]. This different behavior of the two different constituents, called kinematic incompatibility, induces tensile stresses in the matrix, resulting in crack formation [32,39]. This aspect is expected to be more evident for bigger aggregates.

Since SSP contained a higher content of aggregate ranging from 1.18 to 4.75 mm than NS (see Fig. 2), thermal incompatibility is expected to be more severe in the former, this resulting in higher micro-cracks and a lower compressive strength after exposure to high temperature. It was found that thermal cracks were less in number but more opened in the mortar mix with 100% SSP after exposure to 600 °C (Fig. 13), which underline the role of the aggregate size.

Regarding the effect of w/c, the reduction of strength due to heating was lower for the mortar with a higher w/c ratio. The strength difference was more evident in the range 250–600 °C, as shown in Fig. 12b and c. The reduction in strength with respect to virgin conditions for w/c ratios of 0.30 and 0.50 at 600 °C was 50% and 47% for 100% NS and 66% and 63%, accordingly, for 100% SSP.

3.4.2. *Residual porosity*

The residual porosity of mortar mixes exposed to elevated temperatures is shown in Fig. 14. For all mixes, porosity monotonically increases with temperature. At 120 °C, a sharp increase in porosity was found for all mortar mixes, about 1.4–1.5 times higher than the porosity at ambient temperature. As discussed in Section 3.4.1, this behavior is linked to the rising pore volume resulting from the evaporation of capillary water and part of the physically adsorbed water [32]. At 250 °C, porosity increases with almost the similar slope of the range 20–120 °C for mortar mixes made with a w/c ratio of 0.30, while a milder slope was observed for w/c ratio of 0.50. These results confirm the measurements of compressive strength in the same range of temperatures.

Above 400 °C, a notable increase in porosity was found for all mixes,

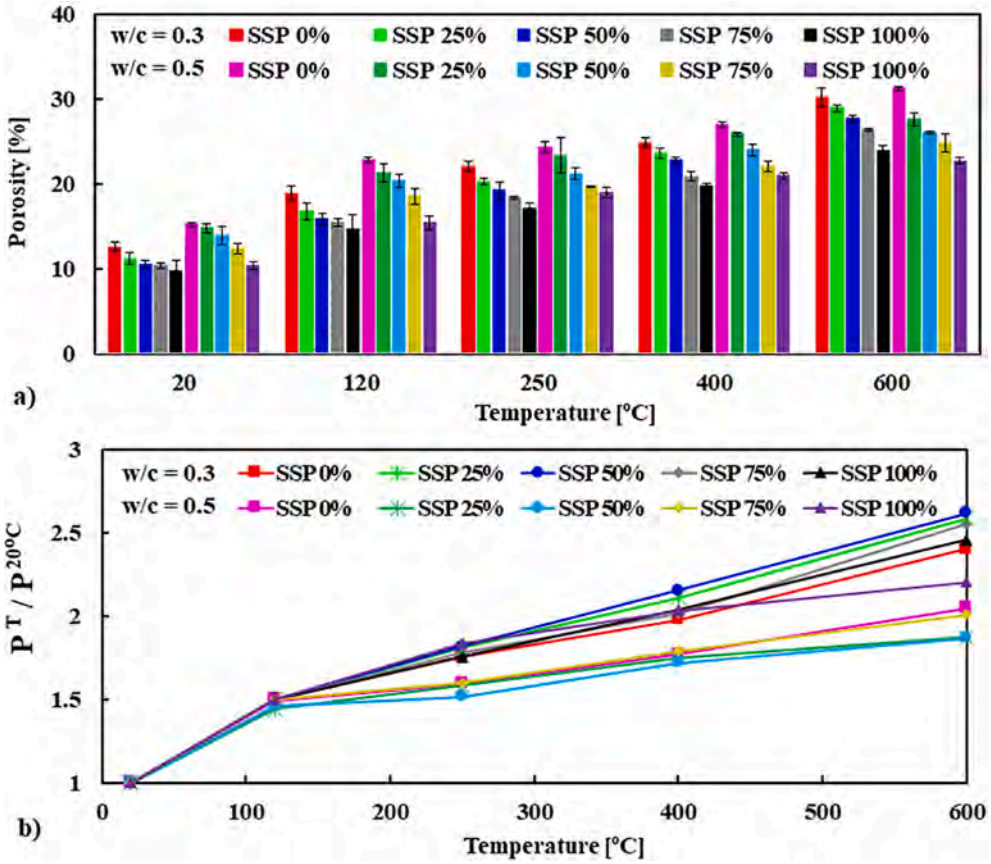

Fig. 14. Residual porosity (P) of mortar after being exposed to elevated temperatures.

which could be attributed to a remarkable increase in the average pore size in the mortar matrixes. This higher porosity satisfactorily agrees with the results on compressive strength at higher temperatures (Fig. 12). It is noted that a higher increase in porosity was observed for the mortar made with a lower w/c ratio compared to higher w/c, which agrees with the residual compressive strength of mortar mixes made with those two w/c ratios.

4. Conclusions

In the present study, the effects of steel slag powder (SSP) as a partial/full replacement of natural sand (NS) is investigated, addressing physico-mechanical properties of cementitious mortar at ambient after exposure to high temperature. Five different replacement levels of NS with SSP have been considered (namely, 0, 25, 50, 75 and 100%) for two values of w/c ratios (0.3 and 0.5). At ambient temperature, porosity, water capillary absorption, chlorides penetration, on the one hand, and compressive, tensile and flexural strengths, on the other hand, have been studied. In residual conditions, namely after exposure to 120, 250, 400 and 600 oC, compressive strength and total porosity have been assessed.

Based on the experimental evidence and of the discussion on the results, the key finding of the present study can be reported as follows:

1. Decreasing workability of mortars was observed as SSP relative content increased, with a slump reduction of around 35–36% when the NS was entirely replaced.
2. Compressive, tensile and flexural strengths increased as SSP content increases due to the denser microstructure, rougher surface texture and angular shape of SSP particles and improved ITZ. Such increase reached the values of 45%, 72% and 56% for compressive, tensile, and flexural strength, respectively, when SSP entirely replaces NS.
3. Porosity, water absorption, and chloride penetration were significantly reduced for increasing percentages of SSP, thanks to the denser microstructure. Porosity, water absorption, and chloride penetration decreased by 42%, 61% and 52%, respectively, when NS was entirely replaced.
4. The higher the SSP contents, the lower the mortar autogenous shrinkage, thanks to the lower water absorption and the higher angularity of the SSP particles (this latter aspect fosters a more effective restrain against the matrix contraction).
5. The residual compressive strength monotonically decreased with the maximum temperature reached in the thermal cycle. The decrease was significantly higher when SSP entirely replaced NS. Conversely, residual porosity increased with temperature, which is consistent with the results on residual compressive strength. The worst behavior at high temperature in a mortar with SSP can be ascribed to the denser microstructure, fostering higher pore pressure during heating and higher thermal stresses, both aspects inducing a more severe crack pattern.

The findings of this study reveal that SSP can be used as a full replacement of NS, thanks to its improved mechanical properties, shrinkage, and durability, even though a slightly worse behavior has been observed after exposure to high temperature. This high strength (compressive strength at 28 days ≈ 70 MPa) cementitious mortar made with SSP could be used in the ferrocement technique/repair work, providing higher strength, better bond, and higher durability of strengthened structural elements as ferrocement has a lower net cover and the higher surface area of the reinforcement (i.e., higher risk of corrosion). Besides, SSP mortar gives environmental benefits by solving the disposal problem, reducing the demand for new fine aggregate, and leading to sustainable construction building materials.

Declaration of Competing Interest

The authors declare that they have no known competing financial interests or personal relationships that could have appeared to influence the work reported in this paper.

Acknowledgements

The authors are grateful to the Department of Civil Engineering, the University of Asia Pacific for the financial support and assistance were given to this research project. A special thanks to Md. Munir Hossain Patoary for performing part of the tests, in partial fulfillment of his Master's degree requirements.

References

[1] Mehta PK, Monteiro PJ. Concrete microstructure, properties and materials; 2017.
[2] Domone P, Illston J. Construction materials: their nature and behaviour. CRC Press; 2010.
[3] Nedeljković M, Visser J, Nijland TG, Valcke S, Schlangen E. Physical, chemical and mineralogical characterization of Dutch fine recycled concrete aggregates: A comparative study. Constr Build Mater 2021;270:121475. https://doi.org/10.1016/j.conbuildmat.2020.121475.
[4] Jiang Yi, Ling T-C, Shi C, Pan S-Y. Characteristics of steel slags and their use in cement and concrete—A review. Resour Conserv Recycl 2018;136:187–97.
[5] Roychand R, Kumar Pramanik B, Zhang G, Setunge S. Recycling steel slag from municipal wastewater treatment plants into concrete applications–A step towards circular economy. Resour Conserv Recycl 2020;152:104533. https://doi.org/10.1016/j.resconrec.2019.104533.
[6] Miah M, Miah MS, Sultana A, Shamim TA, Alom MA. The Effect of Steel Slag Coarse Aggregate on the Mechanical and Durability Performances of Concrete. Key Engineering Materials: Trans Tech Publ; 2020. p. 228-32.
[7] Khalaf MA, Ban CC, Ramli M, Ahmed NM, Sern LJ, Khaleel HA. Physicomechanical and gamma-ray shielding properties of high-strength heavyweight concrete containing steel furnace slag aggregate. J Build Eng 2020;30:101306. https://doi.org/10.1016/j.jobe.2020.101306.
[8] Pan Z, Zhou J, Jiang X, Xu Y, Jin R, Ma J, et al. Investigating the effects of steel slag powder on the properties of self-compacting concrete with recycled aggregates. Constr Build Mater 2019;200:570–7.
[9] Qasrawi H, Shalabi F, Asi I. Use of low CaO unprocessed steel slag in concrete as fine aggregate. Constr Build Mater 2009;23(2):1118–25.
[10] Santamaría-Vicario I, Rodríguez A, Gutiérrez-González S, Calderón V. Design of masonry mortars fabricated concurrently with different steel slag aggregates. Constr Build Mater 2015;95:197–206.
[11] Devi VS, Gnanavel BK. Properties of concrete manufactured using steel slag. Procedia Eng 2014;97:95–104.
[12] Guo Y, Xie J, Zhao J, Zuo K. Utilization of unprocessed steel slag as fine aggregate in normal-and high-strength concrete. Constr Build Mater 2019;204:41–9.
[13] Guo Y, Xie J, Zheng W, Li J. Effects of steel slag as fine aggregate on static and impact behaviours of concrete. Constr Build Mater 2018;192:194–201.
[14] Olonade KA, Kadiri MB, Aderemi PO. Performance of steel slag as fine aggregate in structural concrete. Nigerian J Technol 2015;34(3):452. https://doi.org/10.4314/njt.v34i3.4.
[15] Mohammed N, Arun DP. Utilization of industrial waste slag as aggregate in concrete applications by adopting Taguchi's approach for optimization. Open. J Civil Eng 2012;2012.
[16] Baalamurugan J, Ganesh Kumar V, Chandrasekaran S, Balasundar S, Venkatraman B, Padmapriya R, et al. Utilization of induction furnace steel slag in concrete as coarse aggregate for gamma radiation shielding. J Hazard Mater 2019;369:561–8.
[17] Lo Monte F, Gambarova PG. Thermo-mechanical behavior of baritic concrete exposed to high temperature. Cem Concr Compos 2014;53:305–15.
[18] Miah MJ, Lo Monte F, Felicetti R, Carré H, Pimienta P, La Borderie C. Fire spalling behaviour of concrete: Role of mechanical loading (uniaxial and biaxial) and cement type. Key Eng Mater 2016;711:549–55.
[19] Roy S, Miura T, Nakamura H, Yamamoto Y. High temperature influence on concrete produced by spherical shaped EAF slag fine aggregate–Physical and mechanical properties. Constr Build Mater 2020;231:117153. https://doi.org/10.1016/j.conbuildmat.2019.117153.
[20] Rashad AM, Sadek DM, Hassan HA. An investigation on blast-furnace stag as fine aggregate in alkali-activated slag mortars subjected to elevated temperatures. J Cleaner Prod 2016;112:1086–96.
[21] Miah MJ, Paul SC, Babafemi AJ, Panda B. Strength properties of sustainable mortar containing waste steel slag and waste clay brick: effect of temperature. Materials 2021;14(9):2113.
[22] ASTM C136M-14 Standard test method for sieve analysis of fine and coarse aggregates. ASTM International: West Conshohocken, PA, USA; 2014.
[23] ASTM C33/C33M 18. Standard specification for concrete aggregates. ASTM International: West Conshohocken, PA, USA; 2018.
[24] ASTM. C128-15. Standard Test Method for Relative Density (Specific Gravity) and Absorption of Fine Aggregate. ASTM International: West Conshohocken, PA, USA; 2015.
[25] ASTM. C109/C109M 16a. Standard test method for compressive strength of hydraulic cement mortars (using 2 in. or [50 mm] cube specimens). . ASTM International: West Conshohocken, PA, USA; 2016.
[26] ASTM. C307 18. Standard test method for tensile strength of chemical resistant mortar, grouts, and monolithic surfacings. ASTM International: West Conshohocken, PA, USA; 2018.
[27] ASTM. C348 19. Standard test method for flexural strength of hydraulic cement mortars. ASTM International: West Conshohocken, PA, USA; 2019.
[28] ASTM. C490/C490M 17. Standard practice for use of apparatus for the determination of length change of hardened cement paste, mortar, and concrete. ASTM International: West Conshohocken, PA, USA; 2017.
[29] NFP. p 18–459, Béton-Essai pour béton durci-Essai de porosité et de masse volumique. Mars 2010.
[30] AFREM A. Compte-rendu des journées techniques de l'AFPC-AFREM, Groupe de travail Durabilité des bétons, Méthodes Recommandées Pour la Mesure Des Grandeurs Associées À la Durabilité: 11 Et 12 Décembre 1997. Toulouse.
[31] ASTM. C1202-19. Standard Test Method for Electrical Indication of Concrete's Ability to Resist Chloride Ion Penetration,. ASTM International: West Conshohocken, PA, USA; 2019.
[32] Miah MJ, Kallel H, Carré H, Pimienta P, La Borderie C. The effect of compressive loading on the residual gas permeability of concrete. Construct Build Mater 2019;217:12-9.
[33] van Mier J, Lilliu G. Effect of ITZ-percolation on tensile fracture properties of 3-phase particle composites. Modelling of Cohesive-Frictional Materials: CRC Press; 2007. p. 111-8.
[34] Zhang H, Gan Y, Xu Y, Zhang S, Schlangen E, Šavija B. Experimentally informed fracture modelling of interfacial transition zone at micro-scale. Cem Concr Compos 2019;104:103383. https://doi.org/10.1016/j.cemconcomp.2019.103383.
[35] Guo Z, Jiang T, Zhang J, Kong X, Chen C, Lehman DE. Mechanical and durability properties of sustainable self-compacting concrete with recycled concrete aggregate and fly ash, slag and silica fume. Constr Build Mater 2020;231:117115. https://doi.org/10.1016/j.conbuildmat.2019.117115.
[36] Eurocode 2, 1992-1-2. Design of concrete structures. Part 1–2: General rules – structural fire design. Brussels, Belgium; 2005.
[37] Joint A. TMS Committee 216,". Code Requirements for Determining Fire Resistance of Concrete and Masonry Construction Assemblies (ACI 2161-07/TMS-216-07)," American Concrete Institute, Farmington Hills, MI; 2007.
[38] Miah J. The Effect of Compressive Loading and Cement Type on the Fire Spalling Behaviour of Concrete, Ph.D. Thesis, Université de Pau et des Pays de l'Adour, Pau, France, 19 October; 2017.
[39] Kalifa P, Chéné G, Gallé C. High-temperature behaviour of HPC with polypropylene fibres: From spalling to microstructure. Cem Concr Res 2001;31(10):1487–99.
[40] Bažant ZP. Analysis of Pore Pressure, Thermal Stress and Fracture in Rapidly Heated Concrete. International Workshop on Fire Performance of High-Strength Concrete Proceedings Appendix B: Workshop Papers B101997.
[41] Rossino C, Lo Monte F, Cangiano S, Felicetti R, Gambarova PG. HPC subjected to high temperature: a study on intrinsic and mechanical damage. Key Engineering Materials: Trans Tech Publ; 2015. p. 239-44.
[42] Lo Monte F, Felicetti R, Miah MJ. The Influence of pore pressure on fracture behaviour of normal-strength and high-performance concretes at high temperature. Cem Concr Compos 2019;104:103388. https://doi.org/10.1016/j.cemconcomp.2019.103388.
[43] Seleem HEl_DinH, Rashad AM, Elsokary T. Effect of elevated temperature on physico-mechanical properties of blended cement concrete. Constr Build Mater 2011;25(2):1009–17.